

Efficiency of free auxiliary models in describing interacting fermions: from the Kohn-Sham system to the optimal entanglement model

Kristian Patrick,^{1,*} Marcela Herrera,² Jake Southall,¹ Irene D’Amico,^{3,4,†} and Jiannis K. Pachos^{1,‡}

¹*School of Physics and Astronomy, University of Leeds, Leeds, LS2 9JT, United Kingdom*

²*Centro de Ciências Naturais e Humanas, Universidade Federal do ABC, Avenida dos Estados 5001, 09210-580 Santo André, Sao Paulo, Brazil*

³*Department of Physics, University of York, York, YO10 5DD, United Kingdom*

⁴*Instituto de Física de Sao Carlos, Universidade de Sao Paulo, CP 369, 13560-970, Sao Carlos, Sao Paulo, Brazil*

(Dated: September 18, 2022)

Density functional theory maps an interacting Hamiltonian onto the Kohn-Sham Hamiltonian, an explicitly free model with identical local fermion densities. Using the interaction distance, the minimum distance between the ground state of the interacting system and a generic free fermion state, we quantify the applicability and limitations of the Kohn-Sham model in capturing all the properties of the interacting model. As a byproduct, this distance determines the optimal free state that reproduces the entanglement properties of the interacting system as faithfully as possible. When applied to the Fermi-Hubbard model we demonstrate that in the thermodynamic limit, rather surprisingly, the optimal free state provides an asymptotically exact representation of the ground state for all values of interaction coupling. The proposal of an optimal entanglement model, as the parent model to the optimal free state, opens up the exciting possibility of extending the systematic applicability of auxiliary free models into the non-perturbative and the strongly-correlated regimes.

Undoubtedly, interactions give rise to a wide range of quantum phases of matter with intriguing and exotic properties, ranging from many-body localisation [1] to the fractional quantum Hall effect [2]. Nevertheless, the theoretical investigation of interacting systems is often formidable due to their complexity [3–5]. A possible approach in studying interacting systems is to approximate them by free systems that offer a simpler and intuitive description. To this aim, physicists, chemists and material scientists alike have often used Density Functional Theory (DFT) [6–8]. In its basic formulation, DFT uniquely maps a many-body system to an auxiliary non-interacting one, known as the Kohn-Sham (KS) system [9], which has the same ground state fermion density as the interacting system. While it is known to fail in the strong correlation limit, the KS system has been used to estimate many-body properties other than the fermion density, such as band-structure calculations [8, 10], quantum work [11], and entanglement [12]. However, it is not known how optimal the KS model is within the set of all possible free fermion theories.

To quantify the applicability, in the above sense, of the KS model we employ the concept of interaction distance, $D_{\mathcal{F}}$ [13]. This distance measures how far the ground state of a given system is from the manifold of all free fermion states in terms of their quantum correlations, which are responsible for most exotic properties of interacting systems [13–15]. The interaction distance also identifies the optimal free state, a state with entanglement properties as close as possible to the interacting system. We demonstrate that, in the perturbative (weak-interaction) regime, if $D_{\mathcal{F}} \approx 0$ then the KS ground state is close to the optimal free state, with an error in deter-

mining *any* observable of the interacting system bounded by $D_{\mathcal{F}}$. We also show that, away from the perturbative regime the reliability of the KS model as an approximation can fail even if $D_{\mathcal{F}} \approx 0$. Indeed, interactions may “freeze” some fermionic degrees of freedom used to build the KS model. To describe the interacting model as faithfully as possible in all coupling regimes we introduce the “optimal entanglement model”, with a Hamiltonian that has the optimal free state as its ground state. This alternative to the KS model reproduces all the properties of the interacting system, even in the strong-correlation regime, with an error bounded by $D_{\mathcal{F}}$.

To exemplify this approach we employ the Fermi-Hubbard model. By determining its interaction distance we quantify the regimes where the KS and the optimal entanglement models are good approximations to the interacting system and where they fail. Moreover, we numerically demonstrate that at half-filling, and by appropriately approaching the thermodynamic limit, the interaction distance tends to zero for any values of the interaction coupling. Hence, the optimal entanglement model can faithfully reproduce all properties of the Fermi-Hubbard model for all coupling regimes.

Kohn-Sham and Optimal Entanglement Models. Let us consider a Hamiltonian $\hat{H} = \hat{K} + \hat{V} + \hat{W}$ on a lattice, built from a kinetic energy operator \hat{K} , a local potential operator $\hat{V} = \sum_i^L v_i \hat{n}_i$, where \hat{n}_i the site-occupation operator, and a particle-particle interaction operator \hat{W} . At the core of DFT are the one-to-one correspondences between the ground state wave function $|\psi\rangle$, the corresponding ground state density $\langle \hat{n}_j \rangle_{j=1,L}$ and the local potential [16] of an L -site many-body system [10]. With the ansatz of n and v -representability,

these correspondences imply that there exists a unique non-interacting system, the so called Kohn-Sham system [9], which is subject to the same kinetic operator and having the same ground-state density as the original N -particle interacting system. Through this system, the density, and then in principle all other physical many-body properties [8], could be obtained. The KS Hamiltonian is given by $\hat{H}_{\text{KS}} = \hat{K} + \hat{V}_{\text{KS}}$, where the Kohn-Sham potential, \hat{V}_{KS} , is a combination of the original one-body potential, \hat{V} , the Hartree potential representing the classical electrostatic interaction and the exchange-correlation potential. The latter contains contributions from the many-body interactions of the original system. Apart from relatively simple systems, determining the KS model requires approximations [8]. Nevertheless, it remains a significantly simpler task than solving the interacting system.

Let us now consider the entanglement properties of the interacting system. For a given bipartition into a region A and the complement B of its ground state $|\psi\rangle$ we define the interaction distance of the reduced density matrix $\rho^{\text{int}} = \text{tr}_B |\psi\rangle\langle\psi|$ as

$$D_{\mathcal{F}}(\rho^{\text{int}}) = \min_{\rho^{\text{free}} \in \mathcal{F}} D_{\text{tr}}(\rho^{\text{int}}, \rho^{\text{free}}), \quad (1)$$

where $D_{\text{tr}}(\rho^{\text{int}}, \rho^{\text{free}}) = \frac{1}{2} \text{tr} \sqrt{(\rho^{\text{int}} - \rho^{\text{free}})^2}$ is the trace distance metric between the reduced density matrices ρ^{int} and ρ^{free} , and the minimisation is over the whole set \mathcal{F} of possible Gaussian states ρ^{free} [13]. This distance measures how distinguishable a fermionic state is from being free in terms of its ground state correlations through a bipartition. It is often amenable to analytical calculations and it can be numerically evaluated efficiently for 1D interacting systems with DMRG methods [13, 14]. We denote by ρ^{opt} the optimal free density matrix that minimises the trace distance $D_{\text{tr}}(\rho^{\text{int}}, \rho^{\text{free}})$, and thus reproduces the entanglement properties of ρ^{int} as faithfully as possible. Its parent Hamiltonian is generally unknown and may offer complementary information to the KS Hamiltonian that optimises over the local fermion densities.

The trace distance is the maximum trace over all positive operator valued measures [18]. Hence, for any observable \mathcal{O} the interaction distance bounds the difference between the expectation value of any observable with respect to ρ^{int} and ρ^{opt} , i.e.

$$|\langle \mathcal{O} \rangle_{\rho^{\text{int}}} - \langle \mathcal{O} \rangle_{\rho^{\text{opt}}} | \leq C_{\mathcal{O}} D_{\mathcal{F}}, \quad (2)$$

where $C_{\mathcal{O}}$ is a constant that depends only on the operator \mathcal{O} (see Appendices). Let us apply this inequality to the local densities of fermions, $\mathcal{O} = \hat{n}_i$. For a state with reduced density matrix ρ at site i we define $n_{i,\rho} = \langle \hat{n}_i \rangle_{\rho} = \text{tr}(\rho \hat{n}_i)$. The ‘natural’ metric [19], between ρ^{int} and ρ^{opt} , on the metric space of local densities over all sites is given

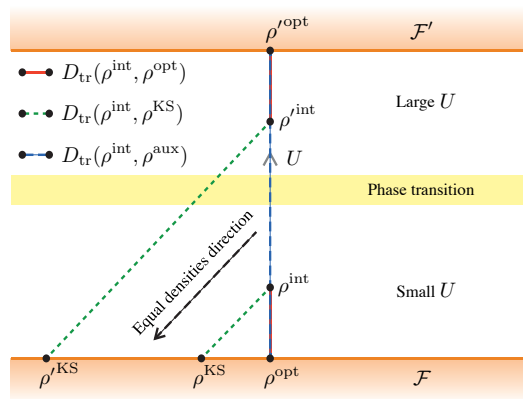


FIG. 1. A schematic illustration of the distances between interacting, ρ^{int} , optimal, ρ^{opt} , and Kohn-Sham, ρ^{KS} , reduced density matrices. Two free manifolds of Gaussian states, \mathcal{F} and \mathcal{F}' , are depicted with possibly different number of degrees of freedom. For small interaction coupling, U , ρ^{int} is close to \mathcal{F} , while as U increases ρ^{int} can be close to another manifold \mathcal{F}' . The direction of equal local fermion densities identifies the KS model on \mathcal{F} . In the perturbative regime (small U), when $D_{\mathcal{F}} \approx 0$, then $D_{\text{tr}}(\rho^{\text{int}}, \rho^{\text{KS}})$ and $D_{\text{tr}}(\rho^{\text{KS}}, \rho^{\text{opt}})$ are also small, as dictated by (5). When U is large then the state ρ^{int} can effectively admit an optimal free description, ρ'^{opt} , with a different number of fermions than the one from the perturbative regime. This change makes the Kohn-Sham model, ρ'^{KS} unsuitable for reproducing the entanglement properties of ρ^{int} .

by

$$D_n(\rho^{\text{int}}, \rho^{\text{opt}}) = \sum_i |n_{i,\rho^{\text{int}}} - n_{i,\rho^{\text{opt}}}|. \quad (3)$$

As the reduced density matrix ρ^{KS} of the KS model has the same local fermion densities as the interacting model we also have $D_n(\rho^{\text{int}}, \rho^{\text{opt}}) = D_n(\rho^{\text{KS}}, \rho^{\text{opt}})$. From Eq. (2) we have then that

$$D_n(\rho^{\text{KS}}, \rho^{\text{opt}}) \leq C D_{\mathcal{F}}, \quad (4)$$

where $C = \sum_i C_{n_i}$. Hence, the interaction distance bounds the density distance between the KS and optimal free model. This bound implies that for $D_{\mathcal{F}} \approx 0$, e.g. in the perturbative regime, the optimal free state has fermion densities that are very close to the densities of the KS ground state.

We now investigate when the KS model reproduces also the entanglement properties of the optimal free model. Assume that the density matrices are a continuous functional of the fermion densities, e.g. when the system is in the perturbative regime with no phase transition caused by the interactions. For small $D_n(\rho^{\text{KS}}, \rho^{\text{opt}})$ we can show that $D_{\text{tr}}(\rho^{\text{KS}}, \rho^{\text{opt}}) \leq c D_{\mathcal{F}}$, for some constant c (see Appendices). Therefore, when the interaction distance is small then ρ^{opt} and ρ^{KS} are nearly overlapping and exhibit very similar entanglement properties. Hence,

for $D_{\mathcal{F}} \approx 0$ the KS model offers a way to constructively obtain the optimal entanglement model.

Let us now employ the triangle inequality of the trace distance metric between the interacting, ρ^{int} , the optimal free, ρ^{opt} , and the KS, ρ^{KS} , reduced density matrices, as shown in Fig. 1. As the interaction distance provides an upper bound for $D_{\text{tr}}(\rho^{\text{KS}}, \rho^{\text{opt}})$ we have $D_{\text{tr}}(\rho^{\text{int}}, \rho^{\text{KS}}) \leq (1 + c)D_{\mathcal{F}}$. Moreover, due to the optimality of ρ^{opt} we have that $D_{\mathcal{F}}$ also lower bounds $D_{\text{tr}}(\rho^{\text{int}}, \rho^{\text{KS}})$, thus giving

$$D_{\mathcal{F}} \leq D_{\text{tr}}(\rho^{\text{int}}, \rho^{\text{KS}}) \leq (1 + c)D_{\mathcal{F}}. \quad (5)$$

Hence, in the perturbative regime when $D_{\mathcal{F}} \approx 0$ the KS model faithfully reproduces all the properties of the interacting system, while a non-zero $D_{\mathcal{F}}$ bounds the errors in determining the entanglement properties of the interacting model. Away from the perturbative regime it is possible that bound (5) fails, by having ρ^{KS} far from ρ^{int} even if $D_{\mathcal{F}} \approx 0$. Nevertheless, ρ^{opt} would still provide a faithful description of ρ^{int} .

The parent Hamiltonian of the optimal free state can be used to define a suitable auxiliary free model, with Hamiltonian H_{aux} and reduced density matrix ρ^{aux} , that identifies the effective degrees of freedom of the interacting model for all coupling regimes. When $D_{\mathcal{F}} \approx 0$ such an auxiliary model not only faithfully reproduces the entanglement properties of the interacting model but, due to Eq. (4), it can also estimate all of its observables, such as the local fermion densities. This ‘optimal entanglement’ model generalises the KS model that, beyond providing exact density, can fail for strong interactions even if $D_{\mathcal{F}} \approx 0$. In fact, strong interactions may not only change the effective local fermion potential, \hat{V} , but also the kinetic term, \hat{K} . To build this auxiliary model one first needs to identify the effective fermionic degrees of freedom that correspond to the quantum correlations of the model. If $D_{\mathcal{F}} \approx 0$ for strong interactions then the number of fermionic degrees of freedom of the emerging free theory can be either the same or smaller than the initial theory without the interaction term: interactions could freeze some of the initial fermionic degrees of freedom but they cannot increase their number. To exemplify this procedure we apply it next to the Fermi-Hubbard model at half-filling.

The Fermi-Hubbard Model. The 1D Hubbard model [20] has successfully reproduced a number of physical phenomena, including interaction-driven quantum phase transitions [21]. In some limits it has exact solutions [22, 23] and has been studied via many numerical techniques including DFT [10]. It comprises spin- $\frac{1}{2}$ fermions with a creation (annihilation) operator $c_{j,\sigma}^{\dagger}$ ($c_{j,\sigma}$) at site j and spin $\sigma \in \{\uparrow, \downarrow\}$, with Hamiltonian

$$H = \sum_{j,\sigma} \left[-J \left(c_{j,\sigma}^{\dagger} c_{j+1,\sigma} + \text{h.c.} \right) + \nu_j n_{j,\sigma} \right] + U \sum_j n_{j,\uparrow} n_{j,\downarrow} \quad (6)$$

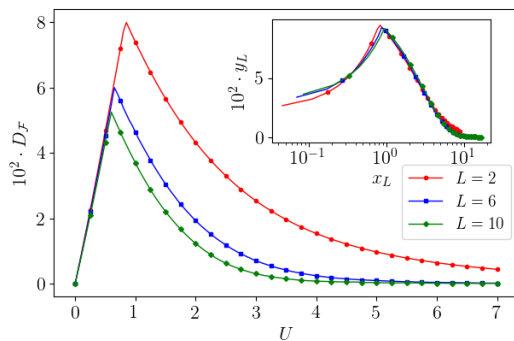


FIG. 2. The interaction distance $D_{\mathcal{F}}$ for the Hubbard model with $J = 1$, all local potentials ν_j being zero except $\nu_1 = 0.5$ and chains of length $L = 2$ (red), 6 (blue), and 10 (green). (Inset) Finite size scaling analysis of $D_{\mathcal{F}}$ with optimal critical exponents $\nu \approx 2.573$, $\zeta \approx 0.243$, and $U_c \approx 0.215$. The collapsed variables are $x_L = (U - U_c)L^{1/\nu}$ and $y_L = D_{\mathcal{F}}L^\zeta$.

where $n_{j,\sigma} = c_{j,\sigma}^{\dagger} c_{j,\sigma}$ is the number operator, J is the tunnelling strength, U is the on-site particle-particle interaction strength, and ν_j is the site-dependent potential. For repulsive interactions, $U > 0$, the model in the thermodynamic limit has two phases: for small U (perturbative regime) it is described by the Luttinger liquid phase, where local fermion densities are free to change, and the large U limit is described by the Mott-insulator phase, where local densities are frozen by Coulomb repulsion [21]. Hence, it is an ideal model to demonstrate the applicability of the optimal entanglement model.

To probe the behaviour of the Hubbard model in the thermodynamic limit we perform a size scaling analysis of the interaction distance. The ansatz used is $D_{\mathcal{F}} \approx L^{-\zeta} f((U - U_c)L^{1/\nu})$, where L is the system size, U_c a critical value of U , f is a smooth function, and ζ , ν are the critical exponents [13]. We consider system sizes of the form $L = 4k + 2$, $k = 0, 1, 2, \dots$ at half filling, where the system has a unique ground state with a symmetric Fermi sea [24]. In Fig. 2 we show both the unscaled value of the interaction distance and the scaling collapse for chains of length $L = 2, 6$, and 10, where the obtained critical exponents are $\nu \approx 2.573$, $\zeta \approx 0.243$, and $U_c \approx 0.215$. Even for these relatively small system sizes the correlation length exponent is consistent with the known CFT result $\nu = 2.5$ [25]. As $\zeta > 0$ the interaction distance decreases with system size, taking the value zero in the thermodynamic limit for all values U . Hence, the interacting model has ground state correlations, and thus a low energy description [26], that can be faithfully represented by free fermions for any value of U . This generalises the known result that the Fermi-Hubbard model is free for large couplings U [21]. In fact, it is possible to construct an auxiliary free model with ground state correlations that converge polynomially fast to the correlations of the interacting model with system

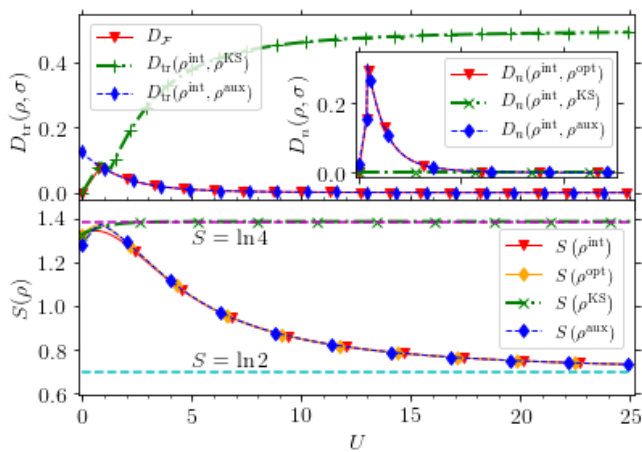


FIG. 3. (Top) Trace distance, (Inset) natural metric, and (Bottom) entanglement entropy for the interacting, ρ^{int} , optimal, ρ^{opt} , KS, ρ^{KS} , and auxiliary, ρ^{aux} , reduced density matrices, as a function of the interaction coupling U , for $L = 2$, $J = 1$, total spin $S_z = 0$, and $\nu_1 - \nu_2 = 0.5$. In the perturbative limit the KS is a good approximation to the optimal entanglement model which describes spin-1/2 free fermions. In the large U limit the KS model fails, while both the optimal and auxiliary states that describe spinless free fermions, provide faithful representations of the local densities (Inset) and the entanglement entropy (Bottom) of the interacting system. For large U the entanglement entropy of the KS model tends to $S = \ln 4$ corresponding to the maximally entangled state $|\psi\rangle = (|\uparrow\downarrow, 0\rangle + |\uparrow, \downarrow\rangle + |\downarrow, \uparrow\rangle + |0, \uparrow\downarrow\rangle)/2$ while the interacting, optimal and auxiliary systems tend to $S \approx \ln 2$ that correspond to $|\psi\rangle = (|\uparrow, \downarrow\rangle + |\downarrow, \uparrow\rangle)/\sqrt{2}$, signalling the freezing of double occupations due to the interactions.

size [27, 28], as shown in the Appendix.

To study in detail the efficiency of the KS and the auxiliary model optimised over entanglement – the optimal entanglement model – in representing the interacting model we focus on the half-filled Hubbard dimer ($L = 2$), that corresponds to the situation farthest from the thermodynamic limit. For this system size both the KS model and the optimal entanglement model can be determined exactly (see Appendices). The behaviour of the corresponding ground state reduced density matrices ρ^{int} , ρ^{KS} , ρ^{opt} , and ρ^{aux} , are given in Fig. 3. Note that $D_{\mathcal{F}} \approx 0$ for all values of U away from the critical region $U_c \approx 1$. Surprisingly, the KS ground state closely approximates the optimal free state not only in the perturbative, but also in the intermediate coupling regime, $U \sim |J|, |\nu_i|$, up to the phase transition region. Here the trace distance between all pairs of states is small, so the KS is both exact in fermion density and also reproduces the ground state correlations of the optimal model accurately. In the strong coupling regime, $U \gg |J|, |\nu_i|$, the KS model fails to reproduce the correlation properties of the interacting model, as it still describes correlations between spinful fermions. In that regime the optimal

free state is described by spinless free fermions. These degrees of freedom faithfully capture the quantum correlations of the interacting model, as shown in Fig. 3 (Bottom). Nevertheless, they only approximate its local densities, as shown in Fig. 3 (Inset), with an error that is bounded by the value of $D_{\mathcal{F}}$, as dictated by Eq. (4).

From the properties of the optimal entanglement model we see that the effect of the strong interactions is to freeze the local fermion populations to $n_j = 1$ as an eigenvalue of the local density operator. This is witnessed by the entanglement entropy where the KS model saturates to the value $S = \ln 4$ due to both spin and population fluctuations, while the interacting model has entanglement entropy that tends to $S = \ln 2$ as $U \rightarrow \infty$, due to only spin correlations. As the interaction distance is approaching zero for large U , we expect that there should exist a free fermion model that can accurately reproduce these spin correlations. To achieve this we construct an auxiliary model that has the optimal free state as its ground state, where the spin degree of freedom is mapped to two non-interacting dimers. We observe that away from the perturbative regime the new auxiliary model faithfully reproduces both the local densities as well as the correlation properties of the interacting system, as shown in Fig. 3 (see Appendices).

Referring back to the schematic in Fig. 1, it is clear that interactions have the effect of moving the optimal free state from the free manifold \mathcal{F} through a phase transition to \mathcal{F}' , where the latter manifold accounts for the reduced fermionic degrees of freedom. Due to the fixed form of the kinetic term of the KS Hamiltonian, its corresponding reduced density matrix will always live in \mathcal{F} . In choosing the auxiliary model that optimises entanglement, we are able instead to reproduce all the properties of the interacting system for all U 's, with an error that is proportional to $D_{\mathcal{F}}$.

Conclusions. With the help of the interaction distance, $D_{\mathcal{F}}$, we are able to identify the free model that approximates the interacting one by optimising over the corresponding entanglement properties. We can demonstrate that when the interaction distance is small then the optimal entanglement model reproduces all observables of the interacting system with accuracy bounded by $D_{\mathcal{F}}$ and it provides an accurate modelling of its low energy behaviour [13, 26]. The KS model, on the other hand, finds local densities exactly for all strengths of interactions, but can dramatically fail to obtain entanglement features even when the interaction distance is small. Motivated by these results we envisage that a method inspired by DFT, where the optimisation of the free model is performed with respect to entanglement properties rather than local densities can faithfully approximate strongly interacting systems.

To exemplify the diagnostic power of the interaction distance, we considered the Fermi-Hubbard model. We numerically demonstrated the surprising result that this

model at half-filling can be represented exactly in the thermodynamic limit ($L = 4k + 2 \rightarrow \infty$) by free fermions for any value of its interaction coupling U . As this model is tractable through the Bethe ansatz [21] it offers the intriguing possibility to determine analytically the optimal entanglement model.

Acknowledgements. We would like to thank Pasquale Calabrese, Konstantinos Meichanetzidis, Chris Turner, and Zlatko Papić for inspiring conversations. Fig. 1 was designed by Jack White. KP, JS, and JKP acknowledge support by the EPSRC grant EP/I038683/1. IDA and MH acknowledges support from the Royal Society through the Newton Advanced Fellowship scheme (Grant no. NA140436) and IDA from CNPq (Grant: PVEProcesso: 401414/2014-0).

* py11kp@leeds.ac.uk

† irene.damico@york.ac.uk

‡ j.k.pachos@leeds.ac.uk

- [1] R. Nandkishore and D. A. Huse, *Con. Mat. Phys.* **6**, 15 (2015).
- [2] R. B. Laughlin, *Phys. Rev. Lett.* **50**, 1395 (1983).
- [3] F. Verstraete, V. Murg, and J. Cirac, *Physics* **57**(2), 143 (2008).
- [4] G. Vidal, *Phys. Rev. Lett.* **101**, 110501 (2008).
- [5] M. P. Nightingale and C. J. Umrigar, *Springer Science & Business Media* **525**, (1998).
- [6] R. O. Jones and O. Gunnarsson, *Rev. Mod. Phys.* **61**, 689 (1989).
- [7] R. O. Jones, *Rev. Mod. Phys.* **87**, 897923 (2015).
- [8] K. Capelle, *Braz. J. Phys.* **36**, 13181343 (2006).
- [9] W. Kohn and L. Sham, *Phys. Rev.* **140**, A1133 (1965).
- [10] K. Capelle and V. L. Campo, *Phys. Rep.* **528**, 91-159 (2013).
- [11] M. Herrera, R. Serra, and I. D’Amico, arXiv:1703.02460.
- [12] J. P. Coe, A. Sudbery, I. D’Amico, *Phys. Rev. B* **77**, 205122 (2008)
- [13] C. Turner, K. Meichanetzidis, Z. Papić, and J. Pachos, *Nat. Comm.* **8**, 14926 (2017).
- [14] K. Meichanetzidis, C. Turner, A. Farjami, Z. Papić, and J. Pachos, arXiv:1705.09983.
- [15] J. K. Pachos and Z. Papić, arXiv:1803.06812.
- [16] J. P. Coe, I. D’Amico and V. V. Franca, *EPL* **110**, 63001 (2015).
- [17] P. Hohenberg and W. Kohn, *Phys. Rev. B* **136**, B846-B871 (1964).
- [18] M. A. Nielsen and I. Chuang, ‘Quantum computation and quantum information,’ (2002).
- [19] I. D’Amico, J. Coe, V. V. Franca, and K. Capelle, *Phys. Rev. Lett.* **106**, 050401 (2011).
- [20] J. Hubbard, *Proc. R. Soc. London, Sec. A* **276**, 238 (1963).
- [21] F. H. Essler, H. Frahm, F. Göhmann, A. Klümper, and V. E. Korepin, *The one-dimensional Hubbard model*, Cambridge University Press, (2005).
- [22] E. Lieb and F. Wu, *Phys. Rev. Lett.* **20**, 1445 (1968).
- [23] J. Carmelo and D. Baeriswyl, *Phys. Rev. B* **37**, 13 (1988).
- [24] F. H. L. Essler, A. M. Läuchli and P. Calabrese, *Phys. Rev. Lett.* **110**, 115701 (2013).
- [25] N. Kawakami and S.-K. Yang, *J. Phys.: Condens. Matter* **3**, 5983 (1991).
- [26] H. Li and F. Haldane, *Phys. Rev. Lett.* **101**, 010504 (2008).
- [27] M. Ogata and H. Shiba, *Phys. Rev. B* **41**, 2326 (1990).
- [28] M. Ogata, T. Sugiyama, and H. Shiba, *Phys. Rev. B* **43**, 8401 (1991).

Bounding observables with $D_{\mathcal{F}}$

It is necessary in this work to compare measurable quantities, such as local density, between the interacting state and optimal free state. In doing so, we arrive at a bounding that relates the interaction distance to the difference between observable expectation values of the interacting and optimal free states. To show this, we compare the expectation value of an observable for two state density matrices ρ and σ . The expectation value of an observable \mathcal{O} can be computed directly through knowledge of the ground state density matrix ρ , i.e. $\langle \mathcal{O} \rangle_{\rho} = \text{tr}[\mathcal{O}\rho]$. In comparing the expectation value of two density matrices, ρ and σ , it is possible to define their difference by the metric

$$d_{\mathcal{O}}(\rho, \sigma) = \left| \langle \mathcal{O} \rangle_{\rho} - \langle \mathcal{O} \rangle_{\sigma} \right| \quad (7)$$

which quickly reduces to $d_{\mathcal{O}} = |\text{tr}[\mathcal{O}(\rho - \sigma)]|$. Let us express $\rho - \sigma$ in its diagonal basis, $(\rho - \sigma) = \sum_k \phi_k |\phi_k\rangle\langle\phi_k|$, where ϕ_k are the eigenvalues of $\rho - \sigma$. Then, via direct substitution into $d_{\mathcal{O}}$, we find that

$$d_{\mathcal{O}} = \left| \text{tr} \left[\mathcal{O} \sum_k \phi_k |\phi_k\rangle\langle\phi_k| \right] \right| \quad (8)$$

$$= \left| \sum_k \langle \phi_k | \mathcal{O} | \phi_k \rangle \phi_k \right| \quad (9)$$

$$\leq \left| \max_k \langle \phi_k | \mathcal{O} | \phi_k \rangle \sum_k \phi_k \right| = C_{\mathcal{O}} \left| \sum_k \phi_k \right| \quad (10)$$

where $C_{\mathcal{O}} = \left| \max_k \langle \phi_k | \mathcal{O} | \phi_k \rangle \right| > 0$. It then follows that

$$d_{\mathcal{O}} \leq C_{\mathcal{O}} \sum_k |\phi_k| = C_{\mathcal{O}} \text{tr} |\rho - \sigma| \quad (11)$$

where the final equality explicitly contains the definition of the interaction distance when $\sigma = \rho^{\text{opt}}$. Therefore, when $\rho = \rho^{\text{int}}$ and $\sigma = \rho^{\text{opt}}$ the difference in expectation values are bounded by the interaction distance, i.e.

$$\left| \langle \mathcal{O} \rangle_{\rho^{\text{int}}} - \langle \mathcal{O} \rangle_{\rho^{\text{opt}}} \right| \leq C_{\mathcal{O}} D_{\mathcal{F}} \quad (12)$$

with $C_{\mathcal{O}} = \frac{1}{2} \max_k \langle \phi_k | \mathcal{O} | \phi_k \rangle$ that depends on the operator \mathcal{O} only.

Bounding $D_n(\rho^{\text{KS}}, \rho^{\text{opt}})$ by $D_{\mathcal{F}}$

The result in Eq. (12) can be applied directly to the definition of the natural metric given in Eq. (3) of the main text. Let $P = n_j$ that is the local fermion density at site j within the subspace of the reduced density matrix.

To arrive at the definition of the natural metric we must sum over all sites. Then, Eq. (12) becomes

$$\sum_j C_j D_{\mathcal{F}} \geq \sum_j \left| \langle n_j \rangle_{\rho^{\text{int}}} - \langle n_j \rangle_{\rho^{\text{opt}}} \right|. \quad (13)$$

The right hand side of this equality is precisely the definition of the natural metric and the left hand side consists of a constant $C = \sum_j C_j$ multiplied by the interaction distance. The bound therefore reduces to

$$C D_{\mathcal{F}} \geq D_n(\rho^{\text{int}}, \rho^{\text{opt}}). \quad (14)$$

Due to the key property of the Kohn Sham model, that $\langle n_j \rangle_{\rho^{\text{int}}} = \langle n_j \rangle_{\rho^{\text{KS}}}$, the bound may be cast in terms of the optimal and Kohn Sham ground states

$$C D_{\mathcal{F}} \geq D_n(\rho^{\text{KS}}, \rho^{\text{opt}}). \quad (15)$$

Therefore, when $D_{\mathcal{F}} \approx 0$ the optimal free state shares the same local fermion densities as the interacting and Kohn Sham ground states.

Trace distance bounding in perturbative limit

Here we prove that within the perturbative limit, i.e. when $n_F = n + \delta n$, with n_F the ground state density of the optimal free state, n the ground state density of the interacting/KS model, and δn a small linear response, then $D_{\text{tr}}(\rho^{\text{opt}}, \rho^{\text{KS}}) \leq c \cdot D_{\mathcal{F}}$, with $c > 0$. First consider the limit $\delta n \rightarrow 0$. In this limit $D_{\text{tr}}(\rho^{\text{opt}}, \rho^{\text{KS}}) \rightarrow 0$ and $D_{\mathcal{F}} \rightarrow 0$, so that the inequality above is satisfied by the equality $0 = c \cdot 0$. Next, consider the linear response to be small and non-zero. We have already shown that the density metric is bound by the interaction distance. In DFT, any property of a pure state interacting system described by a Hamiltonian $H = \hat{K} + \hat{W} + \hat{V}$, can be written as a functional of the system ground state density. So, in particular, the (non-diagonal) density matrix elements can also be written as a functional of the ground state density, leading to

$$D_{\text{tr}}(\rho^{\text{opt}}, \rho^{\text{KS}}) = D_{\text{tr}}[n_F, n] = D_{\text{tr}}[\delta n, n]. \quad (16)$$

For small δn , we can approximate $D_{\text{tr}}(\rho^{\text{opt}}, \rho^{\text{KS}})$ around δn :

$$\begin{aligned} D_{\text{tr}}(\rho^{\text{opt}}, \rho^{\text{KS}}) [\delta n, n] &= D_{\text{tr}}[0, n] + \frac{\delta D_{\text{tr}}}{\delta n} \Big|_{\delta n=0} \delta n \\ &+ \frac{\delta^2 D_{\text{tr}}}{\delta n^2} \Big|_{\delta n=0} (\delta n)^2 + \dots \end{aligned} \quad (17)$$

So that

$$D_{\text{tr}}(\rho^{\text{opt}}, \rho^{\text{KS}}) [\delta n, n] \approx \frac{\delta^2 D_{\text{tr}}}{\delta n^2} \Big|_{\delta n=0} (\delta n)^2 > 0 \quad (18)$$

where inequality holds due to $\delta n = 0$ being a minimum (and the trace distance being a metric). Similarly, we can approximate the density metric about the minimum:

$$D_n(\rho^{\text{opt}}, \rho^{\text{KS}}) = D_n(\rho^{\text{opt}}, \rho^{\text{KS}})[\delta n, n] \quad (19)$$

$$\approx \left. \frac{\delta^2 D_n}{\delta n^2} \right|_{\delta n=0} (\delta n)^2 > 0 \quad (20)$$

Using Eq.'s (18) and (20), and up to higher orders than $(\delta n)^2$ in δn , we can then write

$$D_{\text{tr}}(\rho^{\text{opt}}, \rho^{\text{KS}})[\delta n, n] \approx \frac{\delta^2 D_{\text{tr}}}{\delta n^2} \Big|_{\delta n=0} \left(\frac{\delta^2 D_n}{\delta n^2} \Big|_{\delta n=0} \right)^{-1} \cdot D_n(\rho^{\text{opt}}, \rho^{\text{KS}}), \quad (21)$$

resulting in

$$D_n(\rho^{\text{opt}}, \rho^{\text{KS}}) = D_{\text{tr}}[\delta n, n] \frac{\left. \frac{\delta^2 D_n}{\delta n^2} \right|_{\delta n=0}}{\left. \frac{\delta^2 D_{\text{tr}}}{\delta n^2} \right|_{\delta n=0}}. \quad (22)$$

Using Eq. (15) we obtain

$$D_{\text{tr}}(\rho^{\text{opt}}, \rho^{\text{KS}}) \leq \frac{\left. \frac{\delta^2 D_{\text{tr}}}{\delta n^2} \right|_{\delta n=0}}{\left. \frac{\delta^2 D_n}{\delta n^2} \right|_{\delta n=0}} \cdot CD_{\mathcal{F}}, \quad (23)$$

where the ratio of second derivatives is a functional of n , but for a given n it will be a number greater than zero that can be represented by the function $f(n) = \frac{\left. \frac{\delta^2 D_{\text{tr}}}{\delta n^2} \right|_{\delta n=0}}{\left. \frac{\delta^2 D_n}{\delta n^2} \right|_{\delta n=0}}$. We then finally obtain

$$D_{\text{tr}}(\rho^{\text{opt}}, \rho^{\text{KS}}) \leq f(n) \cdot CD_{\mathcal{F}}. \quad (24)$$

Exact optimal free state for a four level system

By careful consideration of the interaction distance, we may obtain a full analytical solution for the optimal free state entanglement levels, and for $D_{\mathcal{F}}$ itself, for a four level system, ρ^{int} . A system of N single-particle entanglement levels, $\{\epsilon_j\}$, has $2^N \times 2^N$ dimensional entanglement Hamiltonian, H_E^f , with 2^N levels in the many-body entanglement spectrum, $\{E_j\}$. Therefore, a free spectrum with four many-body levels has two single-particle levels, ϵ_1 and ϵ_2 , that build the full spectrum. It is convenient to work with probability densities, $\rho^{\text{opt}} = e^{-H_E^f}$, allowing the single-particle energies to be defined as: b_1 and b_2 . The free many-body spectrum can then be built in the following way:

$$\begin{aligned} \rho_1^{\text{opt}} &= \left(\frac{1}{2} + b_1\right) \left(\frac{1}{2} + b_2\right) & \rho_2^{\text{opt}} &= \left(\frac{1}{2} - b_1\right) \left(\frac{1}{2} + b_2\right) \\ \rho_3^{\text{opt}} &= \left(\frac{1}{2} + b_1\right) \left(\frac{1}{2} - b_2\right) & \rho_4^{\text{opt}} &= \left(\frac{1}{2} - b_1\right) \left(\frac{1}{2} - b_2\right) \end{aligned}$$

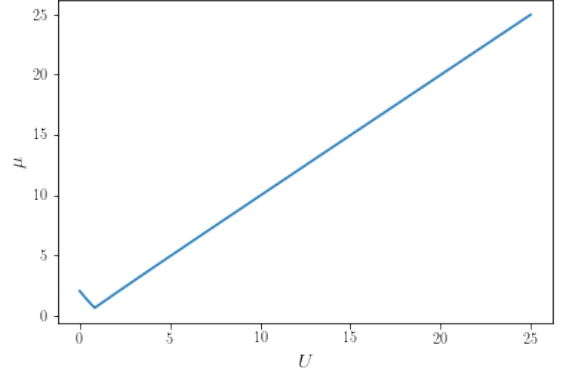


FIG. 4. Scaling of the chemical potential μ , for the $L = N = 2$ optimal entanglement model, against interaction strength of the interacting model, U . In the strong interaction regime we find $\mu = U$ to a very good approximation.

To ensure the spectrum is normalised these levels are subject to $\sum_i \rho_i^{\text{opt}} = 1$, along with $0 \leq b_1 \leq b_2 \leq \frac{1}{2}$ which fixes the ordering to ordering of interacting spectrum: $0 \leq \rho_4^{\text{opt}} \leq \rho_3^{\text{opt}} \leq \rho_2^{\text{opt}} \leq \rho_1^{\text{opt}} \leq 1$.

As a first attempt to minimise the interaction distance one may directly differentiate Eq. (1) of the main text, having substituted in the definitions above, to find the turning points for some choice of parameters b_1 and b_2 ; these parameters contain all of the information required to build the free many body entanglement spectrum. So it is our goal to find the set that minimises $D_{\mathcal{F}}$. In doing so, we find that the derivatives are not defined in the regions $\rho_j^{\text{opt}} = \rho_j^{\text{int}}$ for any j . We also find that second derivatives are always zero when $\rho_j^{\text{opt}} \neq \rho_j^{\text{int}}$, thus defining a saddle point and not a minimum. The minimum trace distance must therefore live on one of the boundary curves $\rho_j^{\text{opt}} = \rho_j^{\text{int}}$ or an intersection of two or more curves.

This analysis yields the following set of solutions for the interaction distance, where the superscript "int" has now been dropped on all ρ_j^{int} :

$$D_{\mathcal{F}} = 2\sqrt{\rho_1} - 2\rho_1 - \rho_2 - \rho_3 \quad \text{if } \rho_1 \geq (\rho_1 + \rho_2)^2 \quad (25)$$

$$D_{\mathcal{F}} = \left| \frac{\rho_1 \rho_4 - \rho_2 \rho_3}{\rho_1 + \rho_2} \right| \quad \text{otherwise.} \quad (26)$$

and the following set of free parameter solutions:

$$b_1 = \sqrt{\rho_1} - \frac{1}{2}, \quad b_2 = \sqrt{\rho_1} - \frac{1}{2} \quad \text{if } \rho_1 \geq (\rho_1 + \rho_2)^2 \quad (27)$$

$$b_1 = \frac{\rho_1 - \rho_2}{2(\rho_1 + \rho_2)}, \quad b_2 = \rho_1 + \rho_2 - \frac{1}{2} \quad \text{otherwise.} \quad (28)$$

These exact solutions allow for an accurate study of the interaction distance without any error of numerical optimisation.

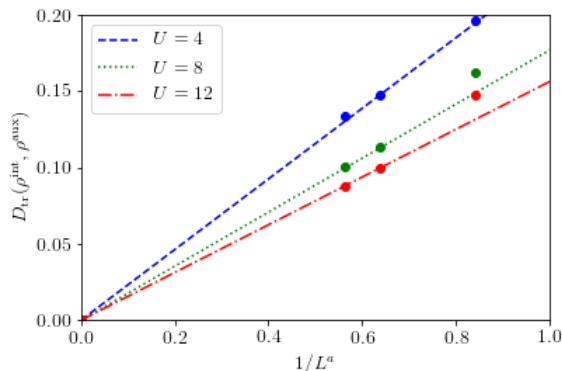


FIG. 5. The trace distance $D_{\text{tr}}(\rho^{\text{int}}, \rho^{\text{aux}})$ for H_{aux} , given in Eq. (31), at half-filling with varying $L = 2, 6, 10$ and $J = 1$, $c = 1$, and $U = 4$ (blue), $U = 8$ (green), $U = 12$ (red). The scaling exponent is $a = 0.25$. We observe that even for these relatively small system sizes $D_{\text{tr}}(\rho^{\text{int}}, \rho^{\text{aux}}) \rightarrow 0$ as $L \rightarrow \infty$; with the $L = 2$ point (far right) showing deviation due to its small size.

An optimal entanglement model for the Hubbard Dimer at half-filling

In order to exemplify the construction of a free auxiliary model that is accurate (within the error of $D_{\mathcal{F}}$) in not only local fermion density but also all other properties, we restrict ourselves to the Hubbard dimer at half filling. The Hilbert space is spanned by the basis $\{|\uparrow\downarrow, 0\rangle, |\uparrow, \downarrow\rangle, |\downarrow, \uparrow\rangle, |0, \uparrow\downarrow\rangle\}$, where the basis state $|x, y\rangle = |x\rangle \otimes |y\rangle$ corresponds to x fermions at the first site and y fermions at the second. In this basis the Hamiltonian, Eq. (6) of the main text, in matrix form is

$$H = \begin{pmatrix} U + 2\nu_1 & -J & J & 0 \\ -J & \nu_1 + \nu_2 & 0 & -J \\ J & 0 & \nu_1 + \nu_2 & J \\ 0 & -J & J & U + 2\nu_2 \end{pmatrix}. \quad (29)$$

Eigenstates of this Hamiltonian have both occupation and spin degrees of freedom that can be varied by tuning the tunnelling and repulsive interaction strength. By observation of the optimal free state entanglement spectrum in the insulating phase, found using the exact solutions quoted previously, it can be seen that there exists a double degeneracy. In order to reproduce this optimal free entanglement spectrum, we construct an auxiliary model with two spinless non-interacting fermions hopping on separate two site chains. By allowing the fermions to hop freely it is possible to obtain an entanglement entropy of

$S = \ln 4$. Then, by appropriately tuning a chemical potential on a single occupation as interactions increase, it is possible to match exactly the double degeneracy of the optimal free entanglement spectrum, as the entropy reduces to $S = \ln 2$ (see Fig. 3 of the main text). Such a spectrum can be reproduced by the following Hamiltonian:

$$H_{\text{aux}} = -\left(c_1^\dagger c_3 + c_3^\dagger c_1\right) - \left(c_2^\dagger c_4 + c_4^\dagger c_2\right) - \frac{\mu}{2} c_1^\dagger c_1 \quad (30)$$

where $\mu = 2 \left[\sqrt{\frac{\rho_1^{\text{opt}}}{\rho_2^{\text{opt}}}} - \sqrt{\frac{\rho_2^{\text{opt}}}{\rho_1^{\text{opt}}}} \right]$ and $(\rho_1^{\text{opt}}, \rho_2^{\text{opt}})$ are the two distinct optimal entanglement levels. The partition that returns the desired spectrum separates sites 1, 2 into subsystem A and sites 3, 4 into subsystem B .

It can be easily seen that $\mu = \mu(U)$ as the optimal free entanglement levels are functions of the interaction strength. Further, as seen in Fig. 4, we observe a linear behaviour $\mu \approx U$ within the insulating phase.

A Free Parent Hamiltonian for the Hubbard Model in the TD Limit

It is possible to construct a free Hamiltonian that reproduces the ground state properties of the Hubbard model in the $L = 4k + 2 \rightarrow \infty$ limit, for any choice of interaction strength U . To see this we refer to Fig. 2 of the main text where the finite size scaling collapse indicates that $D_{\mathcal{F}} \rightarrow 0$ for $L \rightarrow \infty$. In [27, 28], it is shown that a parent Hamiltonian may be constructed from non-interacting spinless fermions with both nearest neighbour and next-nearest neighbour hopping terms that depend on the tunnelling, J , and interaction strength, U , of the interacting Hamiltonian in Eq. (6):

$$H_{\text{aux}} = -J \sum_{j=1}^{L-1} \left(c_j^\dagger c_{j+1} + c_{j+1}^\dagger c_j \right) - \frac{c}{2U} \sum_{j=1}^{L-2} \left(c_j^\dagger c_{j+2} + c_{j+2}^\dagger c_j \right) \quad (31)$$

In Fig. 5, $D_{\text{tr}}(\rho^{\text{int}}, \rho^{\text{aux}})$ is calculated, where ρ^{aux} is the ground state reduced density matrix of H_{aux} satisfying $N/L = 1$. For each value of U the distance scales polynomially with system size due to finite size effects. However, it is clear that in the limit $L \rightarrow \infty$, $D_{\text{tr}}(\rho^{\text{int}}, \rho^{\text{aux}}) \rightarrow 0$ for any choice of U .